

SUPPLEMENTAL MATERIAL:

**Soluble amyloid β oligomers affect dielectric membrane properties by bilayer
insertion and domain formation: Implications for cell toxicity**

Gintaras Valincius,¹ Frank Heinrich,^{2,3} Rima Budvytyte,¹ David J. Vanderah,⁴ Duncan J. McGillivray,⁵ Yuri Sokolov,⁶ James E. Hall,⁶ and Mathias Lösche^{2,3,*}

¹Department of Bioelectrochemistry and Biospectroscopy, Institute of Biochemistry, Vilnius, LT-08662, Lithuania

²Physics Department, Carnegie Mellon University, Pittsburgh, PA 15213-3890

³Center for Neutron Research, National Institute of Standards and Technology, Gaithersburg, MD 20899-6102

⁴Chemical Sciences and Technology Laboratory, National Institute of Standards and Technology, Gaithersburg, MD 20899-8313

⁵Department of Chemistry, The University of Auckland, Auckland 1142, New Zealand

⁶Department of Physiology and Biophysics, School of Medicine, University of California at Irvine, Irvine, CA 92697

This file presents Figs. 2–4 of the main paper in color and provides confidence limit estimates by Monte Carlo resampling for the model parameters describing the data shown in Fig. 2.

*Correspondence:

Mathias Lösche,
Physics Department, Carnegie Mellon University, 5000 Forbes Ave., Pittsburgh, PA 15213-3890
412-268-2735, fax: 412-268-8252, emb: quench@cmu.edu

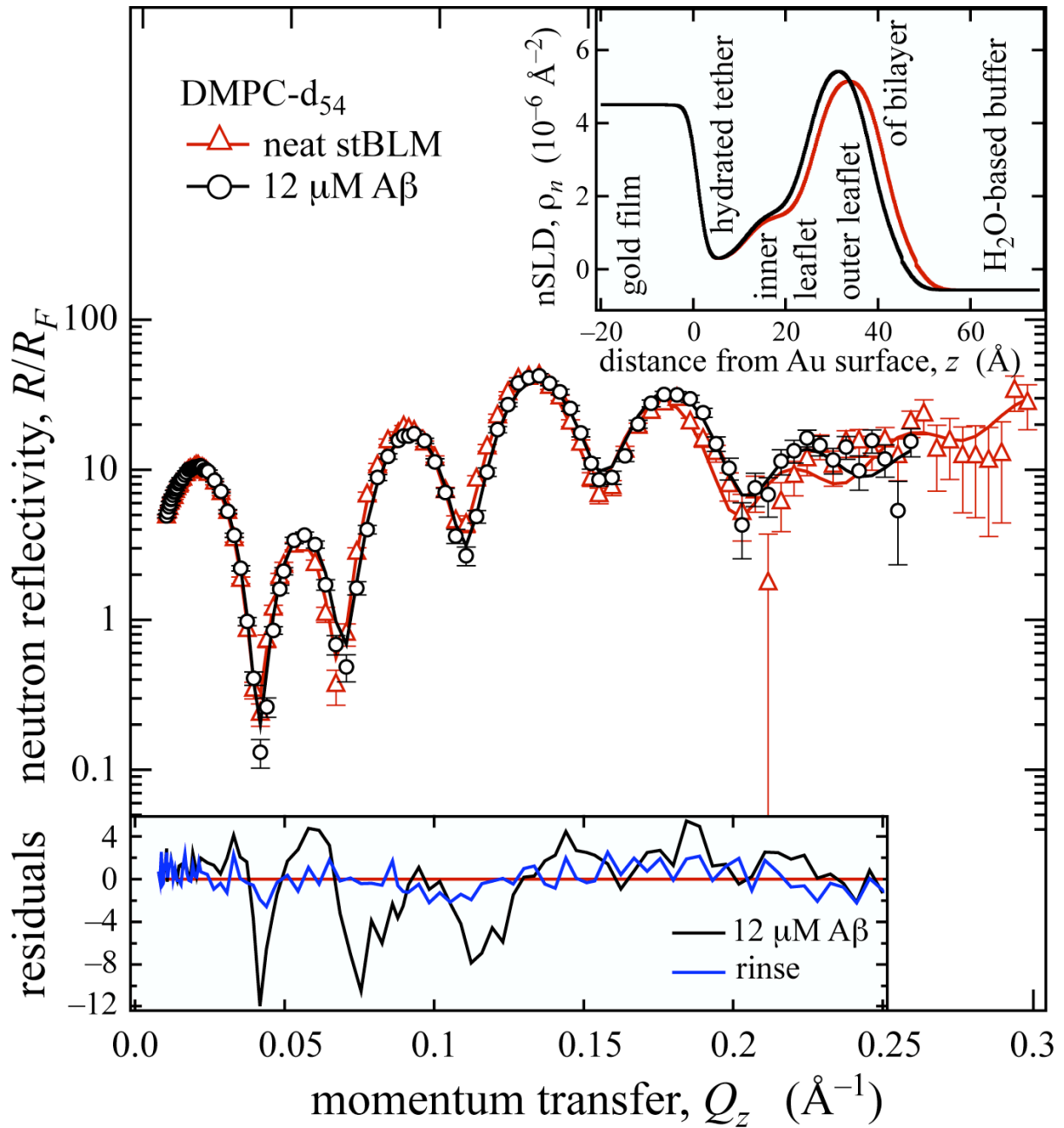


Figure 2 (main paper):

Neutron reflection of an stBLM (WC14: $\beta\text{ME} = 3:7 + \text{DMPC-d}_{54}$), and changes in bilayer structure introduced by $A\beta_{1-42}$ oligomers.

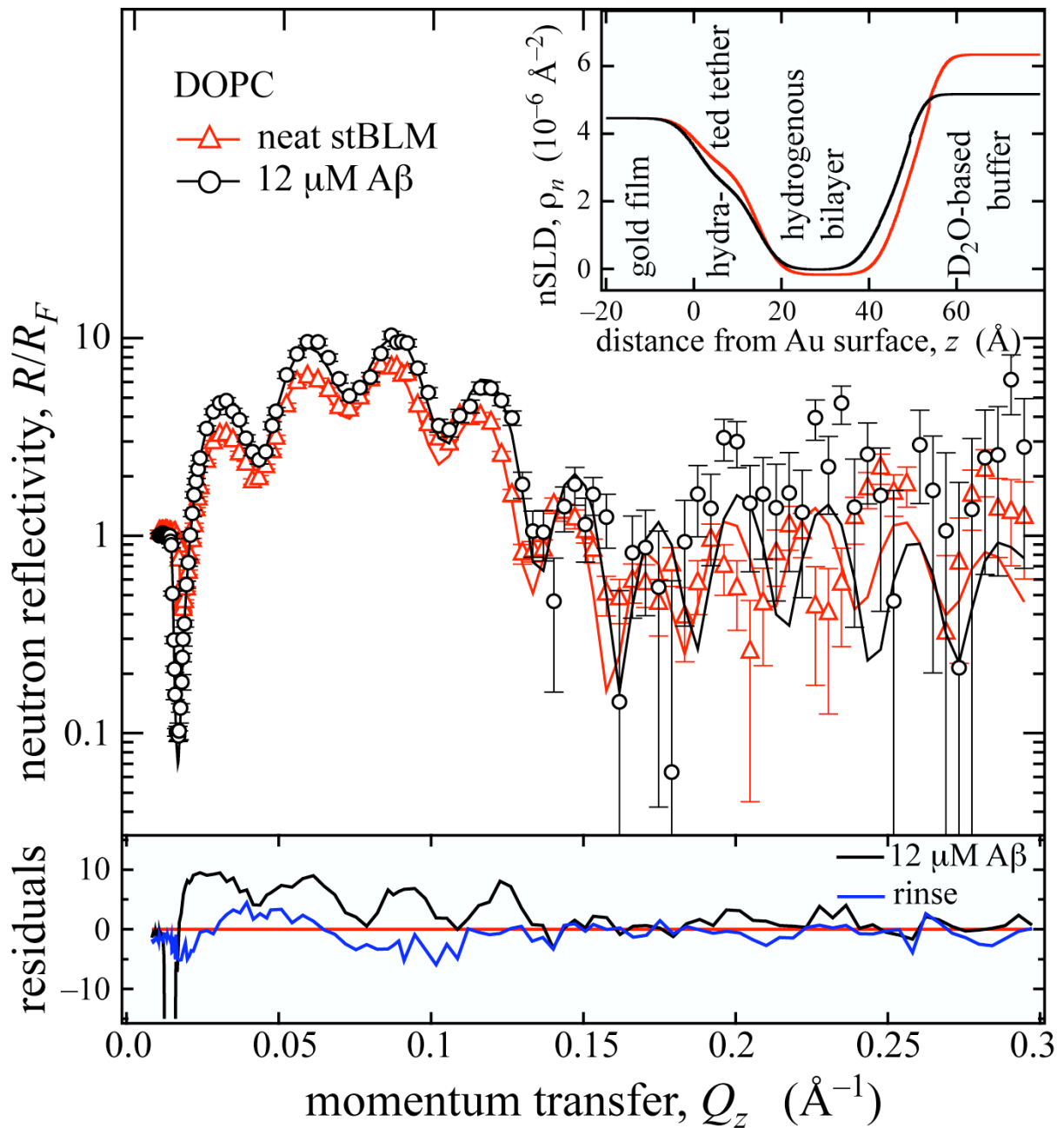


Figure 3 (main paper):

Neutron reflection of an stBLM (WC14: β ME = 3:7 + DOPC), and changes in bilayer structure introduced by $A\beta_{1-42}$ oligomers.

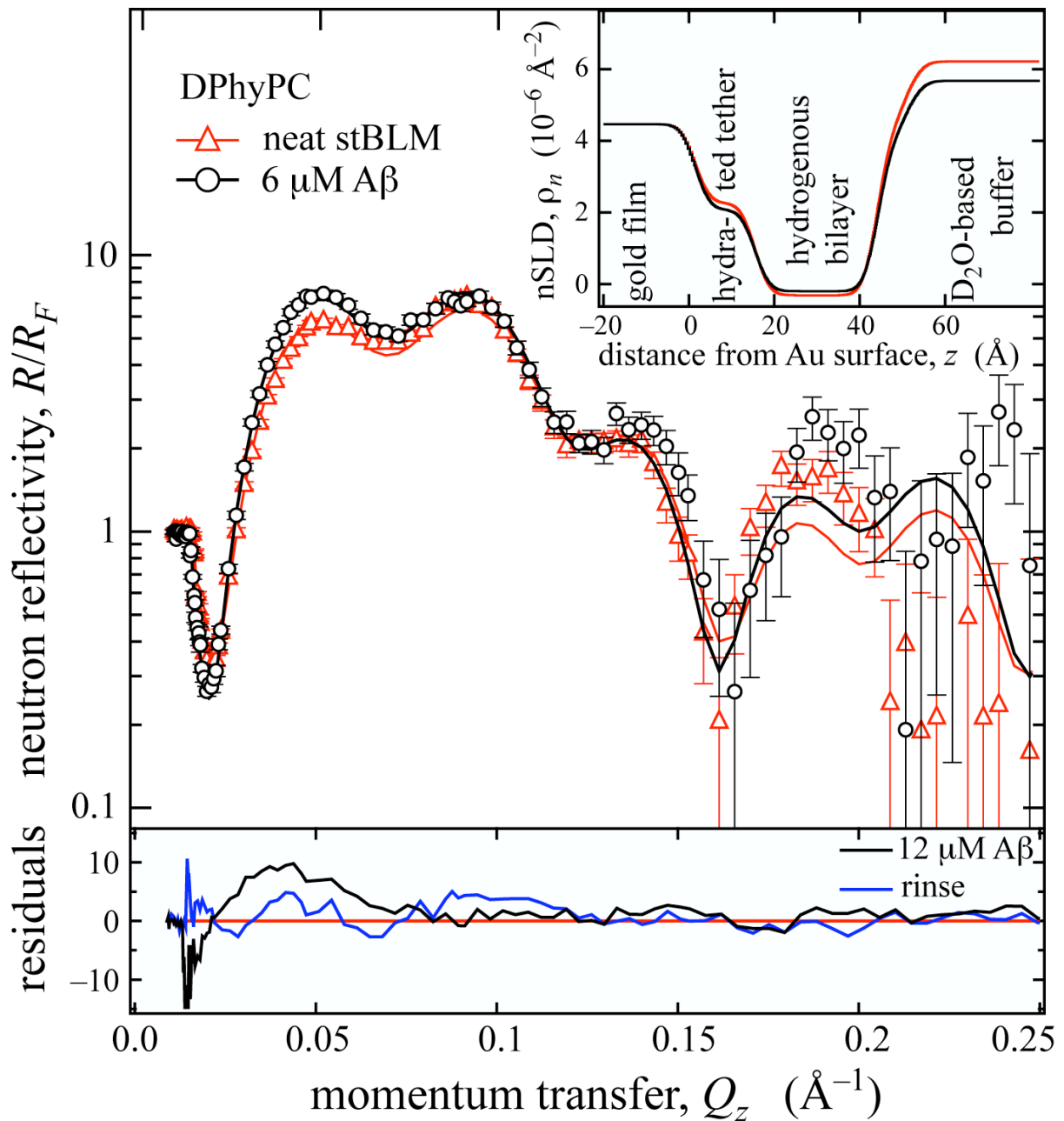


Figure 4 (main paper):

Neutron reflection of an stBLM (WC14:βME = 3:7 + DPhyPC), and changes in bilayer structure introduced by $A\beta_{1-42}$ oligomers.

FULL DESCRIPTION: Full account of the neutron reflectivity model describing the data reported in Table 1 and Fig. 2, and confidence limit estimates by Monte Carlo resampling.

Table 1 in the paper reports the structure of the organic interface layer for a stBLM sample completed with DMPC-d₅₄. Various solvent contrasts were consecutively measured with neutron reflection for the as-prepared membrane (3 solvent contrasts), 2 μ M A β ₁₋₄₂ (2 solvent contrasts), 6 μ M A β ₁₋₄₂ (3 solvent contrasts), 12 μ M A β ₁₋₄₂ (2 solvent contrasts), and after rinse in peptide-free buffer (3 solvent contrasts). The full data set therefore contained 13 individual neutron reflection scans. The sample preparation, solvent exchange, peptide incubation, and rinsing steps were all performed *in situ* on the sample stage of the neutron spectrometer, so that consecutive scans were performed on *exactly* the same footprint of *one* physical sample. Table 1 in the paper reports the best-fit model parameters and their confidence values estimated from the covariance matrix of the final nonlinear Levenberg-Marquardt algorithm.

Best-fit model parameters were determined in a *composition-space refinement* procedure, in which the structure was parameterized in terms of chemical composition (1). The sample structure was evaluated in a complex slab model (2) comprising the following layer sequence:

- the semi-infinite Si substrate
- an oxide layer (SiO_x): ~ 15 Å
- a Cr bonding layer: ~ 15 Å
- an Au film: ~ 100 Å
- a HEO tether layer (containing thiols, β ME, PC headgroups proximal to the substrate, and hydration water): ~ 10 Å
- 2 alkane monolayers of different nSLDs (accounting for different compositions—proximal monolayer: WC14 and DMPC-d₅₄; distal monolayer: only DMPC-d₅₄—and allowing for different degrees of completion, with non-alkane material assumed to be water of the appropriate isotopic constitution), but with the same thickness: $2 \times \sim 15$ Å
- a distal PC headgroup layer (including hydration water): 7 Å fixed
- the semi-infinite buffer (of appropriate isotopic composition)

nSLDs and solvent contents of the HEO, alkane and distal headgroup layers were allowed to vary in the model: Either only the isotopic composition of the water was varied (for neutron reflection scans of the same composition with different solvent contrast) or the water content of the HEO, alkane and distal headgroup layers, as well as the alkane scattering length were varied (for neutron reflection scans at different A β ₁₋₄₂ concentrations in the adjacent buffer). Variations in hydration and in alkane nSLD are evaluated as differentials to the as-prepared state of the stBLM. Thicknesses and nSLDs in the inorganic layers (SiO_x, Cr, Au) were constrained to be identical in all 13 individual neutron reflection scans. This is justified because the sequence of 13 individual scans were performed on the same sample, as described above.

We have further analyzed the neutron reflection data evaluation, and have more rigorously determined model parameter confidence values, in a Monte Carlo resampling procedure, see, e.g., chapt. 14.5 of (3): (a) $N = 1,000$ synthetic data sets were “cloned” from the experimental data by creating random, Gaussian-weighted deviations from the true data based on the experimental uncertainty of each experimental data point determined by counting statistics. (b) By coupling these “mock” data sets in the same way as in the determination of the best-fit model (indicated by parameter spreading across the columns in the Table), N slightly different best-fit “mock” parameter sets were determined. (c) The best-fit “mock” parameter sets were binned and analyzed. In most cases, the resulting parameter distributions were well described by Gaussians. Because some distributions showed asymmetric tails, uncertainties are reported at $2\times$ standard variation (2σ), representing $\sim 95\%$ confidence limits. The complete set of best-fit parameters, including those for the inorganic substrate (which is irrelevant for the membrane structure), is given in Table S1.

Generally, the best-fit parameter values determined in the resampling procedure and in the Levenberg-Marquardt refinement of the experimental data are consistent within the uncertainties. Because of asymmetries in the resampling results, the reported best-fit values deviate in some cases in Tables 1 and S1.

The distributions of the membrane-related parameter values, as determined in the resampling procedure, are reported in Figs. S1–3.

Table S1: Model parameters describing changes of an stBLM structure (WC14: β ME = 3:7 + DMPC-*d*₅₄) upon incubation with soluble prefibrillar A β ₁₋₄₂ oligomers, as determined from Monte Carlo resampling.

	neat bilayer	change from neat bilayer	2 μ M A β ₁₋₄₂	6 μ M A β ₁₋₄₂	12 μ M A β ₁₋₄₂	rinse
thickness (nSLD) of oxide layer	13.6 ^{+0.2} _{-0.6} (3.4×10^{-6} Å ⁻²)					
thickness (nSLD) of Cr layer	16.8 \pm 0.3 (4.0×10^{-6} Å ⁻²)					
thickness (nSLD) of Au layer	101.8 ^{+0.3} _{-0.2} (4.5×10^{-6} Å ⁻²)					
thickness of tether layer (Å)	8.8 ^{+1.5} _{-0.3}					
thickness of each bilayer leaflet (Å)	16.15 ^{+0.25} _{-1.15}	change:	+0.05 ^{+0.07} _{-0.03}	+0.61 ^{+0.10} _{-0.08}	-1.54 \pm 0.07	-0.22 ^{+0.07} _{-0.08}
thickness of head group layer (Å)	7.0 (fixed)					
volume fraction of tether in layer	0.68 \pm 0.01					
volume fraction inner lipid leaflet	0.90 ^{+0.03} _{-0.01}	change:	-0.02 \pm 0.01	0.00 \pm 0.01	+0.02 ^{+0.02} _{-0.01}	-0.01 \pm 0.01
volume fraction outer lipid leaflet	0.94 \pm 0.01	change:	+0.01 \pm 0.01	0.00 \pm 0.01	0.00 ^{+0.01} _{-0.02}	+0.01 \pm 0.01
volume fraction outer head group	0.49 ^{+0.08} _{-0.02}	change:	+0.09 ^{+0.01} _{-0.02}	+0.11 ^{+0.02} _{-0.04}	+0.11 ^{+0.02} _{-0.03}	+0.01 ^{+0.02} _{-0.01}
nSLD inner lipid leaflet (10^{-6} Å ⁻²)	1.49 ^{+0.10} _{-0.05}	change:	+0.29 ^{+0.03} _{-0.04}	+0.29 ^{+0.03} _{-0.04}	+0.12 \pm 0.04	+0.05 ^{+0.04} _{-0.03}
nSLD outer lipid leaflet (10^{-6} Å ⁻²)	5.31 \pm 0.03	change:	+0.21 ^{+0.05} _{-0.03}	+0.38 ^{+0.11} _{-0.03}	+0.34 ^{+0.13} _{-0.05}	+0.08 \pm 0.04
roughness (Å)	2.1 ^{+1.8} _{-0.1}					
bilayer roughness (Å)	6.2 ^{+1.6} _{-0.4}					

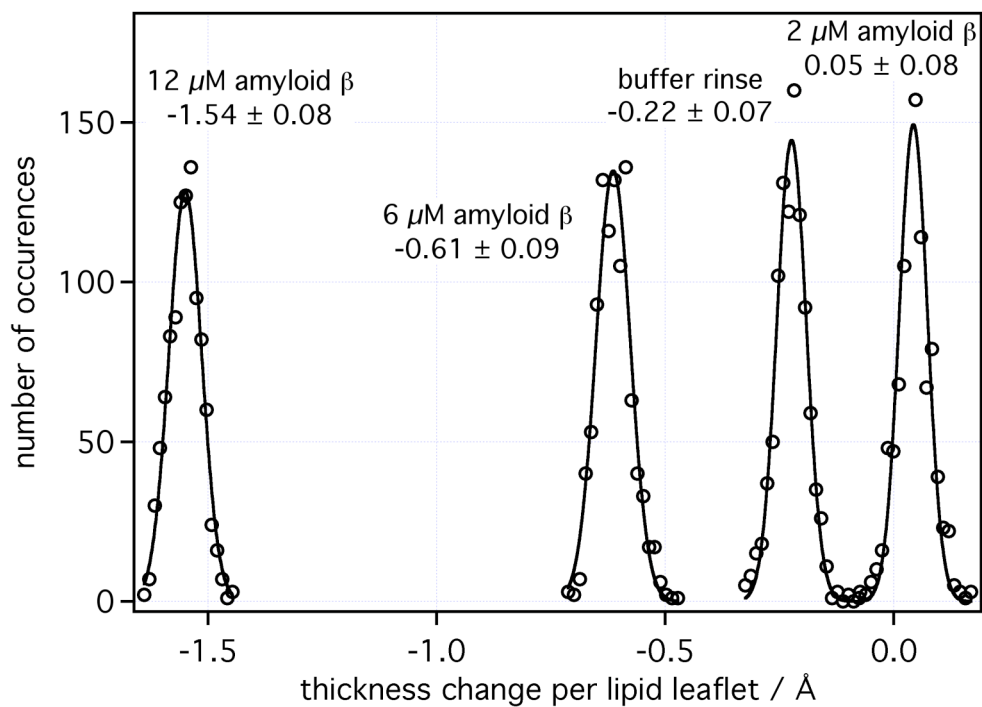


Figure S1: Histograms of best-fit parameter values for thickness changes of the bilayer upon incubation with $A\beta_{1-42}$ obtained from Monte Carlo resampling ($N = 1,000$). Uncertainties report 2 standard deviations.

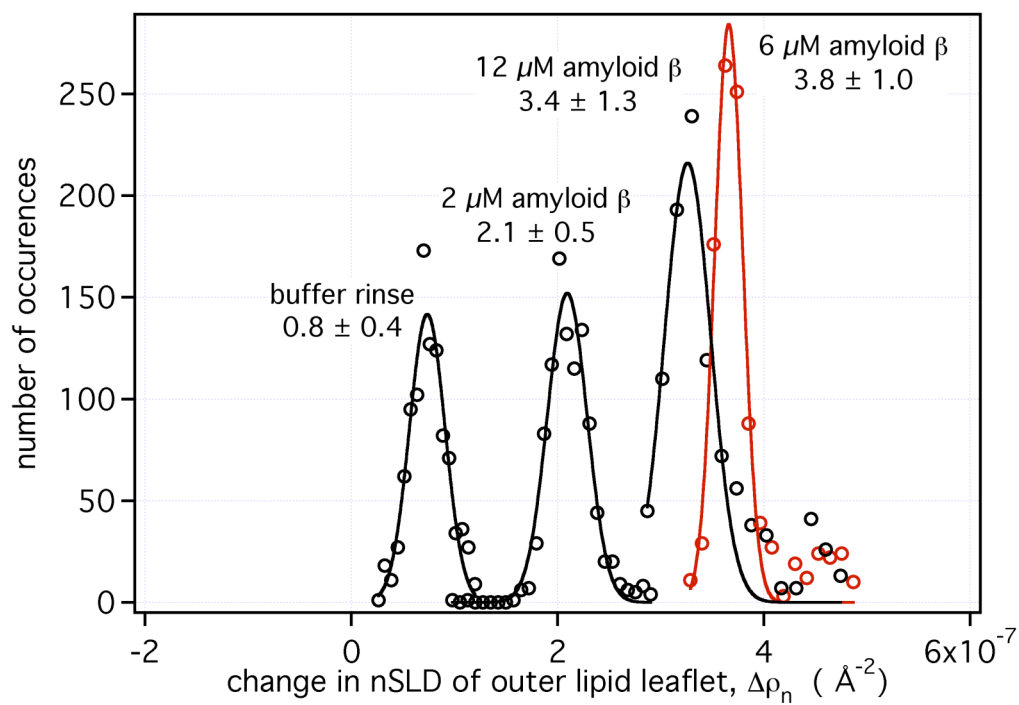


Figure S2: Histograms of best-fit parameter values for nSLD changes of the bilayer distal to the inorganic substrate upon incubation with $A\beta_{1-42}$. Uncertainties report 2 standard deviations.

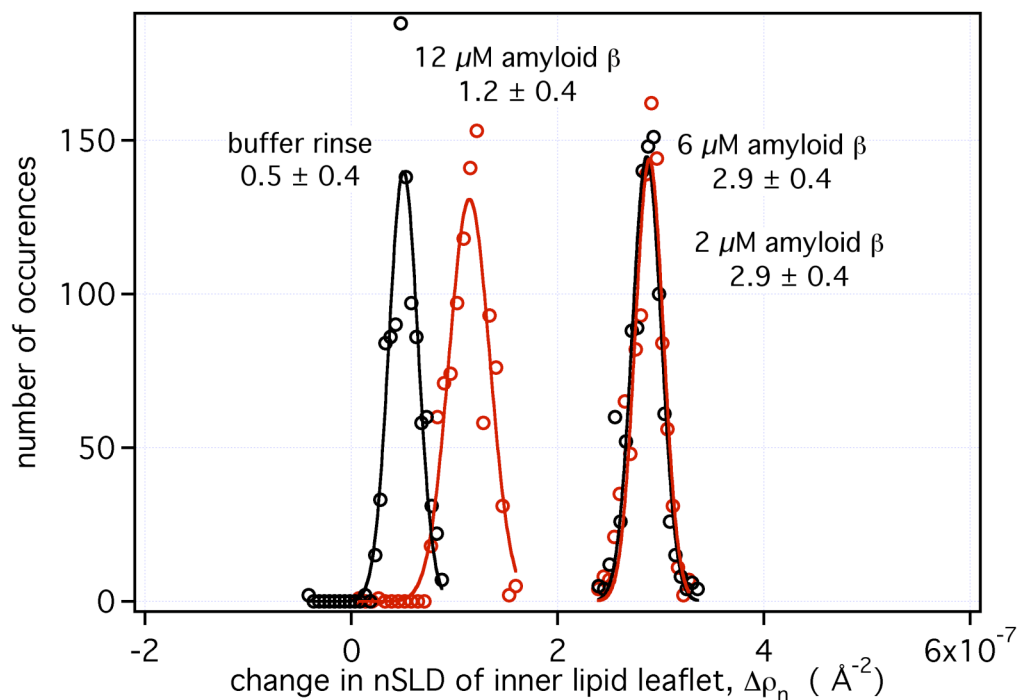


Figure S3: Histograms of best-fit parameter values for nSLD changes of the bilayer proximal to the inorganic substrate upon incubation with $A\beta_{1-42}$. Uncertainties report 2 standard deviations.

REFERENCES

1. Vaknin, D., K. Kjaer, J. Als-Nielsen, and M. Lösche. 1991. Structural properties of phosphatidylcholine in a monolayer at the air/water interface. Neutron reflection study and reexamination of x-ray reflection experiments. *Biophys. J.* 59:1325-1332.
2. Als-Nielsen, J. and K. Kjaer. 1989. X-ray reflectivity and diffraction studies of liquid surfaces and surfactant monolayers. In *Phase Transitions in Soft Condensed Matter*. T. Riste and D. Sherrington, editors. Plenum Press, New York. pp. 113-138.
3. Press, W. H., B. P. Flannery, S. A. Teukolsky, and W. T. Vetterling. 1986. *Numerical Recipes*. Cambridge University Press.